

Sustainability and Mechanical Performance of Fiber-reinforced Self-compacting Concrete (FR-SCC)

A.P. Fantilli ¹, C. Villani ², B. Chiaia ³ and D. Zampini ⁴

ABSTRACT: The performance of fiber-reinforced self-compacting concrete (FR-SCC) under compression are investigated. In general, its ductility is comparable with that of normal vibrated concrete (NC) and self-compacting concrete (SCC) in the presence of confinement. This aspect can be shown by analyzing the mechanical behavior of cylindrical specimens under uniaxial and triaxial compression tests. The post-peak response is defined in terms of $F(w)$, which is a non-dimensional function that relates the inelastic displacement w and the relative stress applied during softening. In the case of SCC, the presence of fibers increases the value of $F(w)$ corresponding to the value of w . Starting from this performance, the mechanical behavior of a low-carbon footprint SCC is also considered. The results of this study indicate that the idea of introducing a new generation of concrete mixtures, capable of maintaining high values of $F(w)$ with a reduced amount of cement, is possible.

1 INTRODUCTION

The production of cement and cement-based composites is not environmental friendly. The impact of concrete industry is mainly due to the clinker, which releases about one ton of carbon dioxide (CO₂) per ton of clinker produced. Evaluating the environmental stress produced by concrete structures during the different phases of life is therefore a basic design requirement (fib, 2010). This is possible by estimating either the energy used for each phase or, equivalently, the CO₂ footprint.

According to Ashby (2009), in the case of concrete structures, 90% of total life-energy is necessary to create the material (i.e. clinker), whereas only 10% is related to the product manufacturing, transportation and use. For these reasons, in order to increase the eco-efficiency of concrete elements, new mix-design procedures aiming at reducing CO₂ emission need to be introduced.

Habert and Roussel (2009) suggest two possible strategies to reach carbon mitigation objectives. The first, generally called material performance strategy, is based on the reduction of clinker by reducing the total amount of concrete, and thus the volume of concrete structures. Obviously, the mechanical performances, such as the compressive strength f_c , need to be increased with respect to classical concrete. It has been estimated that the CO₂ released by the construction of concrete columns can be reduced of about 20%, when f_c increases from 40 MPa to 60 MPa (Habert and Roussel, 2009). Nevertheless, the cost of such enhancement of strength is not always competitive, and frequently high strength concrete can show very brittle mechanical response, especially under compression (Li and Park, 2004).

The second strategy consists in substituting clinker with cementitious and/or pozzolanic mineral admixtures, such as fly ashes and silica fumes (Mehta and Monteiro, 2006). However, also the substitution strategy can be very expensive and the final properties of

¹ Assistant professor, Politecnico di Torino, alessandro.fantilli@polito.it

² Ph.D. Student, Purdue University, cvillani@purdue.edu

³ Professor, Politecnico di Torino, bernardino.chiaia@polito.it

⁴ Dr. Eng., Cemex Research Group SA, davide.zampini@cemex.com

concrete are often not enhanced, particularly in case of poor quality ingredients or poor mixture proportioning.

Both the strategies can suitably be combined in order to reduce the amount of clinker and increase the mechanical strength and ductility of concrete. This is the aim of the present work, in which the mechanical performances and the eco-efficiency of two different self-consolidating concretes (SCC), plain or fiber-reinforced with steel fibers (FR-SCC), are investigated.

2 EXPERIMENTAL PROCEDURE

The mechanical performances are investigated by uniaxial compression tests on SCC cylinders, performed in accordance with the experimental procedure described in the following sections. From such tests, it is possible to define the whole response of SCC, including the strength f_c - which permits other mechanical properties to be evaluated (fib, 2010)- and the post-peak ductility (Fantilli et al., 2011).

2.1 Material properties

Two self-consolidating concretes (named Series 1 and Series 2, respectively) have been investigated. Their constituents are reported in Table 1. In both cases, the self-consolidating concretes have a high water/cement ratio (about 0.7), because of a reduction in the cement content with respect to traditional SCC (Mehta and Monteiro, 2006). However, in the case of Series 2 mixture, fly ash and silica fume were added, and consequently their pozzolanic effect can reduce the global water/binder ratio (to about 0.57). In addition, SCC of Series 2 also contains a Viscosity Modifying Agent (VMA) able to modify the cohesion without significantly altering the fluidity. In this way, SCC is more robust and less sensitive to small variations of constituents.

The two self-consolidating concretes have the same mass per unit volume (2300 kg/m^3) and were used to cast plain and fiber-reinforced cylindrical specimens. In particular, Dramix RC 65/35 BN steel fibers (length $L = 35 \text{ mm}$; diameter $\Phi = 0.55 \text{ mm}$), having hooked ends and indicated with the acronym SF, were added to the self-consolidating concrete of Series 1 in the proportion of 35 kg/m^3 (volume fraction $V_f = 0.45\%$). The same type of fibers were also added to the specimens of Series 2 in the proportion of 39 kg/m^3 (volume fraction $V_f = 0.5\%$).

Table 1 - Composition of self-consolidating concretes (kg/m^3).

Constituents	Series 1	Series 2
Water	180	190
Superplasticizer	4.49	6.7
Cement	245	240
Carbonate filler	380	-
Fine aggregate (0÷4 mm)	910	760
Coarse aggregate (4÷12 mm)	600	1060
Fly Ash	-	65
Silica fume	-	30
Viscosity Modifying Agent	-	0.84

2.2 Test program and specimen details

Fifteen cylinders, of height H and diameter D (Fig.1a), were cast using the self-consolidating concretes reported in Table 1. Eight cylinders were made with the SCC of Series 1 and seven cylinders were made out of Series 2 mixture. The specimens of each series were cast simultaneously in polystyrene form, then cured for one week under identical laboratory conditions, and finally tested one month later. The characteristics of the specimens –indicated with an alphanumeric acronym - are reported in Table 2. In

the acronym, the first digits (S1 or S2) refer to the series of SCC, while the second digits indicate the fiber content (0, 35 or 39 kg/m³).

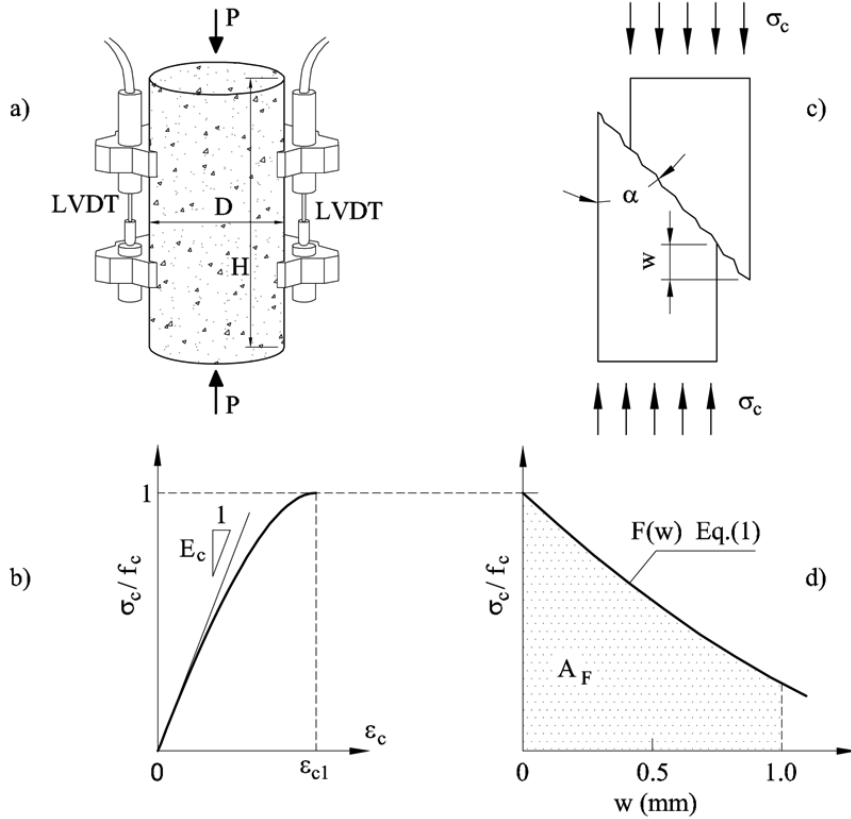


Figure 1 – Uniaxial compressive tests on SCC cylinders: a) geometrical properties and position of the LVDTs; b) pre-peak stress-strain curve; c) the kinematic variables involved in the softening branch; d) post-peak response in terms of $F(w)$ (i.e. relative cohesive stress vs. inelastic shortening w).

Table 2 - The cylindrical specimens tested in uniaxial compression.

Name	H (mm)	D (mm)	Concrete	SF (kg/m ³)
S1_0_1	140	70	Series 1	0
S1_0_2	140	70	Series 1	0
S1_0_3	140	70	Series 1	0
S1_0_4	140	70	Series 1	0
S1_35_1	140	70	Series 1	35
S1_35_2	140	70	Series 1	35
S1_35_3	140	70	Series 1	35
S1_35_4	140	70	Series 1	35
S2_0_1	160	80	Series 2	0
S2_0_2	160	80	Series 2	0
S2_0_3	160	80	Series 2	0
S2_0_4	160	80	Series 2	0
S2_39_1	160	80	Series 2	39
S2_39_2	160	80	Series 2	39
S2_39_3	160	80	Series 2	39

The last number distinguishes the specimens made of the same SCC and the same fiber-reinforcement. The load P was applied vertically through a 1000 kN capacity MTS machine, using the velocity of 0.037 mm per minute. Average deformations were measured over the whole length H , and over a central 50 mm gauge length using two LVDTs (Fig. 1a).

The mechanical response is defined by the stress-strain relationship up to the strength f_c (Fig. 1b), and by the curve $F(w)$ (Fig. 1d), which is the non-dimensional function that relates the inelastic displacement w and the relative stress during softening (Fig. 1c). In this stage, there is the formation of an inclined crack band, which subdivides the specimen into two progressively-sliding blocks. The angle between the vertical axis of the specimen and the sliding surfaces is experimentally found equal to $\alpha \cong 18^\circ$ (Fantilli et al., 2011).

Without going into the details of the post-peak relationship (for a review see Fantilli et al., 2011), it is possible to consider $F(w)$ as a material property defined by the following parabola ($0 \leq w \leq 1$ mm):

$$F(w) = \frac{\sigma_c}{f_c} = 1 + a \cdot w^2 + b \cdot w \quad (1)$$

In the case of normal vibrated concrete (NC) and plain SCC, the values $a = 0.320 \text{ mm}^{-2}$ and $b = -1.12 \text{ mm}^{-1}$ can be adopted. Different values of these coefficients should be introduced in the case of fiber-reinforced concretes.

Within the observed range ($w \sim 0-1$ mm), the ductility in compression can be objectively measured by the area A_F under the curve $F(w)$. Whereas the fracture energy G_{fc} is the product of f_c and A_F and represents the post-peak energy absorption, which is relevant to design against earthquake. In the case of plain NC and SCC, $A_F = 0.55$ mm.

3 TEST RESULTS AND MECHANICAL PERFORMANCES OF SCC AND FR-SCC

Fig.2 reports the stress-strain curves obtained from the specimens of Series 1, plain (Fig.2a) and with steel fibers (Fig.2b), and those of Series 2 without (Fig.2c) and with fiber-reinforcement (Fig.2d).

With respect to the SCC of Series 2, a lower compressive strength f_c and a higher strain ε_{c1} at the peak of stress can be observed in the eight specimens of Series 1, both with and without steel fibers. All the values of f_c and ε_{c1} , which characterize the pre-peak response together with the Young's modulus E_c , are reported in Table 3.

Table 3 - Mechanical properties of the specimens investigated in this project.

Name	f_c (MPa)	E_c (MPa)	ε_{c1} (%)	A_F (mm)
S1_0_1	20.1	17000	0.479	0.554
S1_0_2	28.8	27000	0.504	0.406
S1_0_3	23.2	23000	0.372	0.600
S1_0_4	26.3	25000	0.512	0.638
S1_35_1	24.9	28000	0.323	0.666
S1_35_2	24.7	20000	0.429	0.657
S1_35_3	33.3	15000	0.563	0.698
S1_35_4	34.5	25000	0.611	0.566
S2_0_1	47.8	32000	0.302	0.303
S2_0_2	42.5	29000	0.288	0.272
S2_0_3	46.3	31000	0.275	0.298
S2_0_4	45.3	31000	0.256	0.303
S2_39_1	44.2	30000	0.310	0.622
S2_39_2	44.8	30000	0.288	0.542
S2_39_3	45.8	32000	0.277	0.576

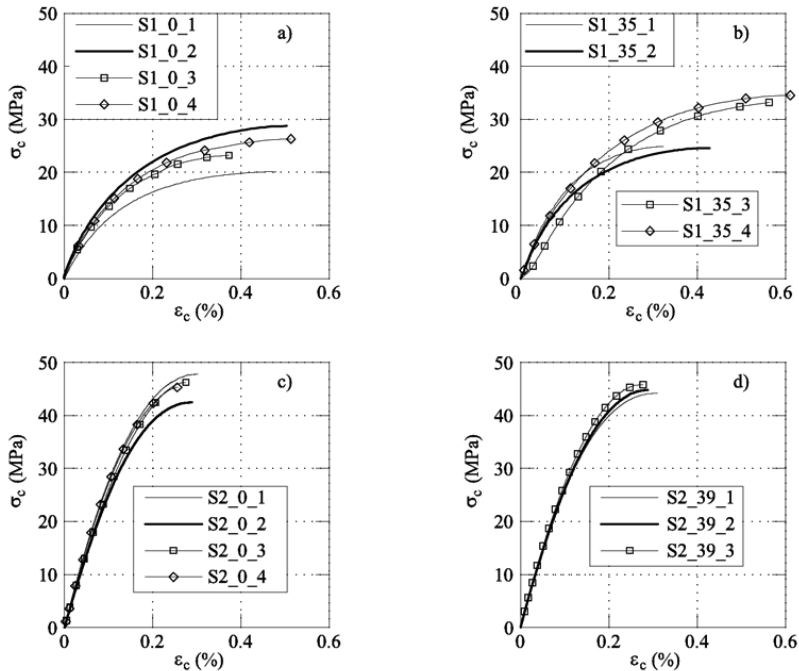


Figure 2 - The σ_c - ε_c curves resulting from tests: a) plain SCC of Series 1; b) Series 1 with 35 kg/m³ of steel fibers; c) plain SCC of Series 2; b) Series 2 with 39 kg/m³ of steel fibers.

As a result, higher stiffness of Series 2 specimens can be observed in the stress-strain curves of Fig.2, corresponding also to the values of E_c (30% higher than those of Series 1 -see Table 3-). Accordingly, the simple reduction of cement content, see, e.g., the specimens of Series 1, leads to the reduction of strength and elastic modulus, whereas the presence of mineral admixture (Series 2) maintains both f_c and E_c unchanged with respect to a traditional concrete or SCC. This is true regardless of fiber content, because f_c , ε_{c1} and E_c generally remain unchanged if the fiber volume fraction is lower than 1%. As both strain localization and diagonal cracks occurred in all the tests, the post-peak stage of SCC and FR-SCC can be described, for all the length and the strength values of the specimens, by the $F(w)$ curves, and by the areas A_F , as previously defined. Such curves are reported in Fig.3 for the specimens of Series 1 without fibers (Fig.3a) and with Dramix RC 65/35 BN (Fig.3b), and those of Series 2 without (Fig.3c) and with fiber-reinforcement (Fig.3d). In the diagrams of Fig.3, the dashed curves represent the behavior of NC as predicted by Eq.(1). All the curves are limited to $w = 1$ mm, in correspondence of which residual compressive stresses vanish in normal vibrated concrete, and the corresponding values of A_F are reported in Table 3.

Eq.(1) provides a good prediction of the post peak response measured in the specimens of Series 1 without fibers (Fig.3a). Conversely, plain SCC of Series 2 shows values of A_F ($\cong 0.3$ mm) remarkably lower than 0.55 mm, which is the value obtained by Eq.(1) within the range $0 \leq w \leq 1$ mm. This difference vanishes in the presence of fiber-reinforcement. Indeed, in all the FR-SCC specimens of Series 1 and Series 2, Eq.(1) correctly predicts both the measured $F(w)$ curves and the corresponding areas A_F (see Table 3). Thus, the beneficial effects produced by steel fibers only regard the post-peak response of the analyzed SCCs. In this way, the specimens of Series 2 reinforced with 39 kg/m³ of steel fibers provide an excellent mechanical performance, as they show

high compressive strength (due to the presence of fly ash and silica fume) and a very ductile softening branch.

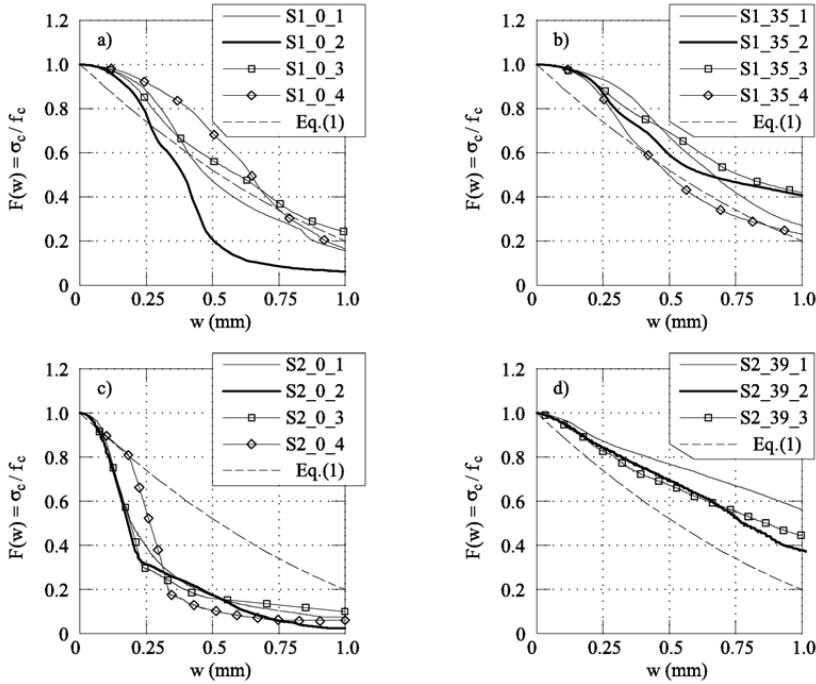


Figure 3 - The $F(w)$ curves resulting from tests: a) plain SCC of Series 1; b) Series 1 with 35 kg/m^3 of steel fibers; c) plain SCC of Series 2; b) Series 2 with 39 kg/m^3 of steel fibers.

4 ECO-EFFICIENCY INDICATORS FOR SCC AND FR-SCC

By introducing new “eco-mechanical” indexes, the environmental impact of SCC and FR-SCC can be estimated and combined with the previous mechanical performances. From a general point of view, these indexes should represent the ratio between the amount of carbon dioxide released to produce certain mixtures of pre-established performance, and the performance itself.

In the pre-peak stage (Fig.2), when the value of performance is simply indicated by the strength f_c , the following index can be introduced:

$$I_{p1} = \frac{Q_{cc} + Q_{cf}}{f_c} \quad (2)$$

where, Q_{cc} = amount of carbon dioxide (measured in kg) necessary to produce the cement used to cast a cubic meter of concrete; Q_{cf} = amount of carbon dioxide (measured in kg) necessary to produce the steel fibers added to a cubic meter of concrete. These quantities can be easily estimated when the constituents of concrete are known (see Table 1 e Table 2), and by assuming that 1 kg and 2.2 kg of CO_2 are released for the production of 1 kg of portland cement and low carbon steel, respectively (Ashby, 2009).

The average values of I_{p1} , computed with Eq.(2) for the analyzed composites (plain SCC of series 1 – S1_0 –, FR-SCC of series 1 – S1_35 –, plain SCC of series 2 – S2_0 –, FR-SCC of series 2 – S1_39 –), are reported in the histogram of Fig.4a. If only the strength f_c is taking into consideration, the SCC of Series 2, with and without fibers,

show the higher eco-efficiency. As a matter of fact, the lowest values of I_{p1} are obtained for the composites S2_0 e S2_39 (Fig.4a).

If the mechanical performances are related to the post-peak stage (Fig.3), and therefore to the area A_F , the eco-mechanical index can be expressed as:

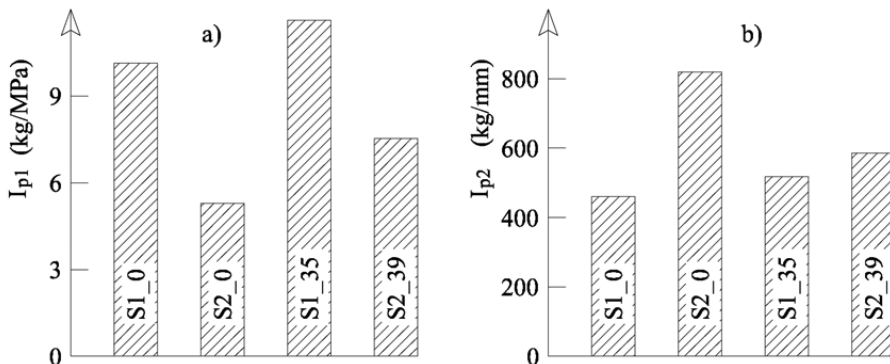


Figure 4 – Eco-mechanical indexes introduced for the SCC and FR-SCC investigated in this project: a) I_{p1} indexes of the pre-peak stage; b) I_{p2} indexes of the post-peak stage.

$$I_{p2} = \frac{Q_{cc} + Q_{cf}}{A_F} \quad (3)$$

The average values of I_{p2} given by Eq.(3) for all the composites tested in the present paper are depicted in Fig.4b. Conversely to the pre-peak stage, the best eco-efficiency is measured for the specimens made with the SCC of Series 1. Specifically, the lowest values of I_{p2} are obtained for the composites S1_0 e S1_35 (Fig.4b). However, it must be remarked that also FR-SCC of Series 2 can provide a good efficiency (see S2_39 in Fig.4b).

When both the pre-peak (Fig.2) and the post peak (Fig.3) responses are taken into consideration, a new global eco-mechanical index can be proposed:

$$I_{tot} = \frac{Q_{cc} + Q_{cf}}{f_c A_F} = \frac{Q_{cc} + Q_{cf}}{G_{fc}} \quad (4)$$

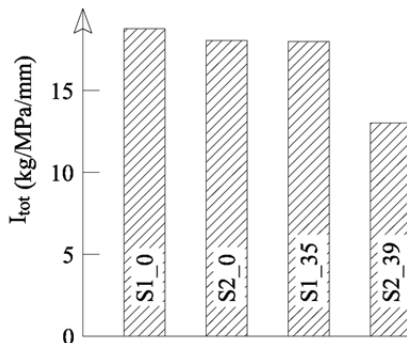


Figure 5 – Evaluation of the global eco-mechanical index I_{tot} for the SCC investigated in this project.

As shown in Fig.5, all the SCCs of Series 1, with and without fibers (S1_35 and S1_0, respectively), and those of Series 2 without fibers (S2_0) show more or less the same $\bar{I}_{tot} \cong 18$ kg/MPa/mm. On the contrary, the FR-SCC of Series 2 (S2_39) shows the lowest $\bar{I}_{tot} = 13$ kg/MPa/mm and, consequently, the best eco-mechanical performances.

5 CONCLUSION

The introduction of eco-mechanical indexes allows the definition of a new strategy to reduce the environmental impact of SCC, without any negative impact on mechanical performance. The theoretical and the experimental analyses developed here indicate that cement content (and thus CO₂ emission) can be reduced in traditional SCC, when the presence of mineral admixtures and fiber-reinforcement provides the same strength and ductility, respectively.

REFERENCES

- Ashby M.F. (2009). “Materials and the Environment: Eco-informed Materials Choice”, Butterworth-Heinemann (Elsevier), London.
- Fantilli A.P., Mihashi H., Vallini P., Chiaia B. (2011) “Equivalent confinement in HPRCC columns measured by triaxial test”, *ACI Materials Journal*, 108(2), 159-167.
- fib (2010). “Model Code 2010 - First complete draft”, *fib Bulletin*, 55.
- Habert G., Roussel N. (2009). “Study of two concrete mix-design strategies to reach carbon mitigation objectives”, *Cement & Concrete Composites*, 31, 397–402.
- Li B., Park R. (2004). “Confining Reinforcement for High-Strength Concrete Columns”, *ACI Structural Journal*, 101(3), 314-324.
- Mehta P.K., Monteiro P.J.M. (2006). “Concrete: Microstructure, Properties, and Materials”, McGraw-Hill Professional, New York.